ORIGINAL CONTRIBUTION

Fabrication of silver-coated PET track-etched membrane as SERS platform for detection of acetaminophen

George Michael Ndilowe[1] · Chris Ademola Bode-Aluko[1] · Deborah Chimponda[1] · Olga Kristavchuk[2] · Iurii Kochnev[2] · Alexander Nechaev[2] · Leslie Petrik[1]

Abstract

In this study, silver nanoparticles (AgNPs) were immobilized on the surface of polyethylene terephthalate (PET) membrane using diethylenetriamine (DETA) as a chemical linker. The molecule of DETA was attached to the surface of PET via an amide bond following scission of the polyester ester bond on the PET surface. The AgNPs were immobilized on the surface of diethylenetriamine-modified PET membrane via a silver-nitrogen covalent bond. The silver-coated, DETA-modified and unmodified PET membranes were characterized by Fourier transform infrared (FTIR), x-ray photoelectron spectroscopy (XPS), ulltraviolet-visible spectroscopy (UV–Vis), and scanning electron microscopy (SEM). The results showed that the size of AgNPs also increased with time of immobilization. The percentage of elemental silver also increased with increase in time of immobilization of AgNPs on the surface of DETA-modified PET membrane. The AgNP-coated PET membrane was used as SERS platform to detect acetaminophen in water. The SERS results showed that acetaminophen molecules could be detected with high Raman scattering intensity arising from adsorption of acetaminophen molecules on the silver nanoparticles of the SERS platform.

Keywords Polyethylene terephthalate · Silver nanoparticles · Surface modifications · Acetaminophen · SERS

Abbreviations

SERS   Surface-enhanced Raman spectroscopy
AgNPs   Silver nanoparticles
PET   Polyethylene terephthalate
DETA   Diethylenetriamine

Highlights • DETA was immobilized on PET track-etched membrane to serves as linker for silver nanoparticles.

   • Silver nanoparticles were immobilized on DETA functionalized PET track-etched membrane to produce SERS membrane.

   • SERS membrane was used to detect acetaminophen using Raman spectroscopy.

✉ Chris Ademola Bode-Aluko
  cbode-aluko@uwc.ac.za

1   Environmental and Nano Sciences Group, Department of Chemistry, University of the Western Cape, Robert Sobukwe Road, Bellville 7535, Republic of South Africa

2   Flerov Laboratories of Nuclear Reactions, Joint Institute for Nuclear Research, Dubna, Moscow Region, Russia 141980

Introduction

Polymeric membranes are organic membranes synthesized from chemically reactive monomers [1, 2]. Polymer membrane materials have various applications in fields such as filtration, biotechnology, microelectronics, coating, thin-film technology, and others which rely on their bulk properties and surface chemistry [3, 4]. Techniques that alter polymer membrane surface properties have attracted the attention of researchers with the aim of immobilizing compounds of interest on the surfaces for various applications [5, 6]. Polymer membranes are inert and therefore lack reactive functional groups on which chemical linkers, metal nanoparticles, and biomolecules could be attached sustainably [7]. The inert nature of most polymer surfaces limits their use in applications; hence, surface modification is required to achieve the desired properties [8]. Amongst high-performance polymer membranes such as polycarbonate (PC), polyimide (PI), and others, polyethylene terephthalate (PET) has good mechanical strength, and thermal and chemical resistance [9, 10]. PET is a linear, aromatic polyester type of organic polymer [11]. PET, an inert polymer, which has not been physically or chemically etched and modified, lacks suitable functional

😗 Springer

groups on the surface therefore the need to chemically modify the surface [10].

The physicochemical modification methods of polymers in some instances are considered as precursors to chemical modification [7]. Chemical modifications such as aminolysis, hydrolysis, amidation, and carboxylation have been used to introduce reactive functional groups on the surface of PET [10]. In an aminolysis reaction, amine nitrogen through its lone pair attacks an electron deficient carbonyl carbon of the ester moiety of PET to form an amide bond [12]. This functionalization is achieved through liquid–solid phase organic synthesis. The organic synthesis provides the most stable covalent bond to immobilize active compounds such as biomolecules and nanoparticles on polymer surfaces [7]. A careful choice of conditions for surface modification should be made to limit degradation of the desirable mechanical and chemical properties of the bulk polymer [13]. The wet chemistry parameters including temperature and time of treatment as well as solvent type and concentration are controlled to maintain consistent surface modification [12]. Irena et al. [14] in a study on PET surface modification observed that aminolysis depended on the choice of amine, temperature, time, and concentration. The chemical linkers are bifunctional so that one terminal group is attached to the metal nanoparticle or biomolecule and the other is coupled to the polymer surface [7]. In another report by Reznickova et al. [8], one thiol terminal end was used to form the silver-sulphur bond and the other was coupled to reactive species on the PET membrane surface. The number of immobilized metal nanoparticles or biomolecules on the modified membrane surface is determined by the available affinity functional groups such as thiols and amines [15]. The choice of the chemical linker, therefore, depends on the chemical properties of the compound to be immobilized [16]. For instance, thiols and amines have a high affinity for noble metal nanoparticles [17]. In a study by Kristavchuk et al. [18], it was observed that increasing the duration of exposure of track-etched polyethylene membrane in a silver dispersion led to increased number of silver nanoparticles on the membrane surface, which was also confirmed visually by changes in appearance.

Nobel metal nanoparticles have many applications in nanotechnology due to their versatility [18]. AgNPs have attracted the attention of researchers due to their good conductivity, chemical stability, anti-bacterial activity, and unique electrical and optical qualities [19]. These nanostructured materials exhibit physical, biological, electrical, and chemical properties that differ substantially from bulk materials [19, 20]. The properties of nanoparticles are dependent on size, shape, and distribution. The nanoparticles have been of interest in the areas of catalysis, photography [20–22] biotechnology, sensing, optics, and surface-enhanced Raman spectroscopy [23–25]. Nanoparticles exhibit enhanced properties compared to bulk properties due to their high surface-to-volume ratio [20].

There is a wide range of applications of surface-enhanced Raman spectroscopy (SERS) as an analytical technique in the fields of biotechnology [26], food industry, warfare anti-terrorism, drug abuse [27], and environmental applications [28], electrochemistry, surface, and material sciences [29]. The SERS technique is of interest in environmental pollutant analysis, with the focus on detecting, identifying, and quantifying very low concentrations of pollutants found either in air or water sources [30]. The driving force behind research and development of SERS is the trace level analysis capability of the technique and its cost effectiveness [31]. The technique also offers good practical utility [2]. SERS has several analytical advantages over other methods including ultra-sensitivity, selectivity, and inherent molecular specificity [26, 32]. Chemical analysis by SERS requires little or no sample preparation [33]. It is also convenient and cost-effective for development of miniaturized equipment [31, 34]. SERS has an edge over infrared spectroscopy, as it can be directly applied in the aquatic environment with negligible background noise due to low polarizability index of water [2]. Although similar techniques such as fluorescence are already well established, the emerging SERS has attractive properties such that it can be used both in the near-infrared and the visible spectral region and does not require labelling the analyte of interest as practiced in the fluorescence technique [35]. The performance of SERS is based on its sensitivity, which depends on the surface property of SERS active materials [36] that can be tailored to suit the intended application [37, 38]. It is envisioned that SERS could be used to simultaneously identify multiple pollutants in a sample reliably, rapidly, and at lower cost [28]. The SERS technique is flexible such that it can be applied in sequence with suitable separation techniques, such as nano filtration polymer membrane technology and chromatography [39], scanning probe microscopy, and microfluidics [35].

The presence of drugs such as acetaminophen in water is known to pose health risk to the aquatic life. Paracetamol (acetaminophen) is a pain reliever and a fever reducer, which is often abused and indiscriminately disposed. In a study done by Rao et al. [40], it was reported that exposure to paracetamol caused behavioural and physical changes in *Cyprinus carpio* (fingerings and adults). These changes include endo- and exo-dermal irritation, discoloration of scales, fin rot, liver muscle, and brain damage which lead to death. It was also observed that low concentrations of paracetamol caused early death in fingerlings compared to adult fish [40].

Therefore, the objective of the study was to develop a quick method of immobilizing AgNPs on the surface of a chemically modified PET membrane for detection of acetaminophen in water. The immobilization will be by means of chemical attachment as opposed to physical method. The

advantage of covalently bonded nanoparticles upon a polymer surface is that they do not leach into the environment. Previously AgNPs have been immobilized on the surface of a glass membrane and on polycarbonate membrane via siloxy linkage [7]. Andrade et al. [41] immobilized AgNPs on the surface of modified glass via (3-aminopropyl)triethoxy silane (APTMS), which was coupled via siloxy linkages. The siloxy linkages functionalized on a modified glass surface used by Andrade et al. [41] were unstable when exposed to some solvent conditions. The siloxy linkage underwent hydrolysis upon exposure to alkaline and high-temperature environments [7]. The approach of this study was to employ diethylenetriamine as a chemical linker on which to directly immobilize AgNPs to the surface of PET membrane soon after chemical modification. The resultant PET membrane coated with AgNPs was used as SERS platform for Raman spectroscopy to detect acetaminophen in water sample at low concentration. It is expected that the silver nanoparticles on the surface would enhance the Raman signal, and therefore generate a more visible and readable spectrum of acetaminophen.

Materials and methods

Chemicals and materials

The track-etched polyethylene terephthalate (PET) membrane (thickness 23 μm, pore density of 1×10^9 cm^{-2} and pore diameter of 0.100 μm) that was obtained from the Joint Institute for Nuclear Research, Dubna, Russia, was used after cleaning in ethanol and distilled water. Diethylenetriamine (DETA) 98%, silver nitrate (AgNO$_3$) 99%, and trisodium citrate 98% were purchased from Alfa Aesar (Germany). Absolute alcohol (EtOH) 99.9% and acetaminophen standard were purchased from Sigma-Aldrich (South Africa). The purchased chemical reagents were used as received. The PET membrane was thoroughly cleaned in a mixture of EtOH and distilled water (1:1 v/v), dried in air, and used without further treatment. All aqueous solutions were prepared using distilled water.

Chemical modification of PET membrane

The surface of the PET membrane was modified by immersing a 2-×2-cm piece of track-etched PET membrane in a 50-mL aqueous solution of diethylenetriamine (DETA) [14]. The aqueous DETA concentrations of 45%, 60%, and 75% (v/v) were used for samples coded 45PET, 60PET, and 75PET, respectively. A 2-×2-cm piece of PET membrane was immersed in each of the concentrations of the aqueous DETA solution. The exposure of PET membranes to the amine solution was carried out at room temperature for

12 h, 18 h, and 24 h. The code CoPET was for a control sample. After subjecting it to the aminolysis reaction, the PET membrane was washed with copious amounts of distilled water and EtOH (1:1 v/v) to remove physically adhered DETA from the surface of the PET membrane. The modified track-etched PET membrane was acid-activated in 1 mM hydrochloric acid for 1 h under agitation at ambient room conditions. The rinsed PET membrane was air-dried at room temperature for 24 h.

Immobilization of AgNPs on PET membrane

A volume of 100 mL solution of aqueous AgNO$_3$ (1 mM) was heated to 90 °C. An aqueous solution of trisodium citrate (1 g/100 mL) of 2 mL was added to the preheated silver nitrate solution followed by immersion of the modified PET membrane [42]. The reduction of silver nitrate was carried out for 0 min, 10 min, 20 min, or 30 min for samples Co-AgPET, 10-AgPET, 20-AgPET, or 30AgPET, respectively. The silver nanoparticle-coated PET membrane was rinsed twice with distilled water to remove physically adsorbed nanoparticles on the surface and air-dried at room temperature for 24 h.

Immobilization of Ag on quartz platform

Quartz surface was prepared by modifying the silicon oxide solid substrate with silver nanoparticles via thermo vacuum and reactive magnetron sputtering. The sputtered silver nanoparticles were of size 30 nm. The silver-coated quartz was used as received from Joint Institute for Nuclear Research (JINR), Dubna, Russia, and is herein code-named Quartz.

SERS detection of acetaminophen using synthesized SERS platform

The detection of acetaminophen using SERS platform (30-AgPET) synthesized in "Immobilization of AgNPs on PET membrane" was carried out at different concentrations of acetaminophen in distilled water. Three concentrations with sample codes in brackets, of 15.1 mg/L (Aceta-100), 1.51 mg/L (Aceta-010), and 0.151 mg/L (Aceta-001) were prepared in 20-μL aliquots. The sample codes are described in Table 1. A 20 μL of acetaminophen was dropped on the surface of a 1-×1-cm piece of the platform and was left to dry under ambient room conditions for 24 h. Afterwards, the platform was placed under the probe of Enspectr R532 model Raman spectrometer for acetaminophen detection.

Characterization of PET membrane and AgNPs

The FTIR spectra of the modified and unmodified track-etched PET membrane samples were obtained using Perkin

Table 1 Experimental parameters and sample codes for detection of acetaminophen using 30-AgPET sample on surface-enhanced Raman spectroscopy (SERS)

	Volume μL	Time (h)	Concentration (mg/L)	Sample code
Acetaminophen	20	24	15.10	Aceta-100
	20	24	1.510	Aceta-010
	20	24	0.151	Aceta-001

Elmer model Spectrum Two spectrometer. The FTIR attenuated total reflectance (ATR) mode was used for surface characterisation. The spectra of the samples were obtained within the range of 3600 to 600 cm^{-1} at a resolution of 4 cm^{-1}. The XPS measurement was performed using a Thermo Scientific K-Alpha X-ray photoelectron spectrometer. The surface morphology of PET membranes was characterized using a Hitachi SU8020 scanning electron microscope. The UV–Vis spectroscopy was done using a Thermo Fisher Evolution 200 spectrometer. The spectral characterisation was performed in a 200- to 600-nm range at room temperature. A Tecnai G2F20 X-Twin MAT 200-kV field emission gun transmission electron microscope was used to characterize the morphology of colloidal AgNPs. Raman spectroscopy was carried out using a portable version of Enspectr R532 Raman spectrometer to study the surface chemistry of unmodified PET, modified PET, SERS platform, and for detection of acetaminophen. The Raman spectrometer is equipped with an internal laser of excitation wavelength 532 nm. The spectrometer is supplied with the objective lens, Olympus CX22 LED of magnification × 10 and × 40. The output power used was 20 mW. The exposure time was set at 600 ms with 20 frames. A manual locator was used to find the spot where to place the sample on the sample holder.

Results and discussion

### Preparation of SERS membrane

Aminolysis of PET

Aminolysis of the PET membrane surface is one of the wet chemistry techniques used to introduce amines on the surface of the polymer membrane via an amide bond. The solid/liquid interface organic reaction involving PET repeat unit on the surface of PET membrane and DETA solution involves scission of the ester bond and formation of amide bond. The schematic mechanism of the aminolysis of PET membrane with DETA and immobilization of AgNPs on the surface of modified surface is presented in Fig. 1a. Figure 1a shows the aminolysis reaction at the solid–liquid interface, a lone pair of electrons on the nitrogen of DETA attack the

partially positive carbon of carbonyl ester. The aminolysis brings about the formation of the amide bond on the surface of the PET membrane between the carboxylic moieties and DETA. Further amide bond formation is from the cleavage of the ester bond that has been facilitated by DETA.

Fourier transform infrared (FTIR) was used to characterize the unmodified and modified PET membrane. The results discussed are those based on concentration after optimizing the time of modification, which was 24 h. The FTIR results in Fig. 1b show that the absorbance peak centred at 2950 cm^{-1} broadens and increases as the concentration of DETA was increased. The absorbance peak at 2950 cm^{-1} is attributed to C-H bond stretching from the ethylene moieties. The partial broadening of the absorbance peak at 3450 cm^{-1} is attributed to N–H stretching. The N–H stretching vibrations are as a result of the amine moieties introduced on the surface from DETA. The absorbance band appearing in the region of 1500–1600 cm^{-1} is observed in the samples 75%DETA, 60%DETA, and 45%DETA which were reacted with aqueous diethylenetriamine at concentrations of 75%, 60%, and 45% respectively. The amide I band appears more pronounced in the spectral region of 1500–1600 cm^{-1}, when the PET membrane was reacted with 75% concentration of DETA.

Similarly, in literature, it was reported that amide I and II bands were observed as a single absorbance peak instead of separate absorbance peaks for a modified track-etched PET membrane that was subjected to aminolysis using other amines such as ethylenediamine [43]. The presence of amide I and II bands on the FTIR spectra of the PET membrane subjected to DETA at different concentrations confirms that the surface of the track-etched PET membrane was modified in each case. Any higher concentration above 75% resulted in cracked and easily torn PET membranes that could not be properly characterized by Fourier transform infrared.

The XPS results in Table 2 show that elemental carbon (C1s) and oxygen (O1s) were present on the surface of unmodified track-etched PET membrane coded 0%DETA, before exposing the membrane to DETA solution in ratio of 2.6 to 1. The sample 75%DETA had a ratio of 3.2 to 1 for elemental carbon to elemental oxygen on the surface of modified PET membrane. The sample 75%DETA shows that the ratio increased for elemental carbon due to the presence of nitrogen (N1s) from DETA that has replaced some oxygen that has been displaced via the aminolysis process, which involves ester bond scission and formation of an amide bond [44]. The elemental compositions are also presented in the general survey graphs of the X-ray photoelectron spectroscopy taken for both PET membrane samples (0%DETA and 75%DETA). The general surveys are shown in Fig. 2a and b. The XPS general surveys show elements within the detection limits based on the chemical composition of the surface of the track-etched PET membrane. The general survey graphs
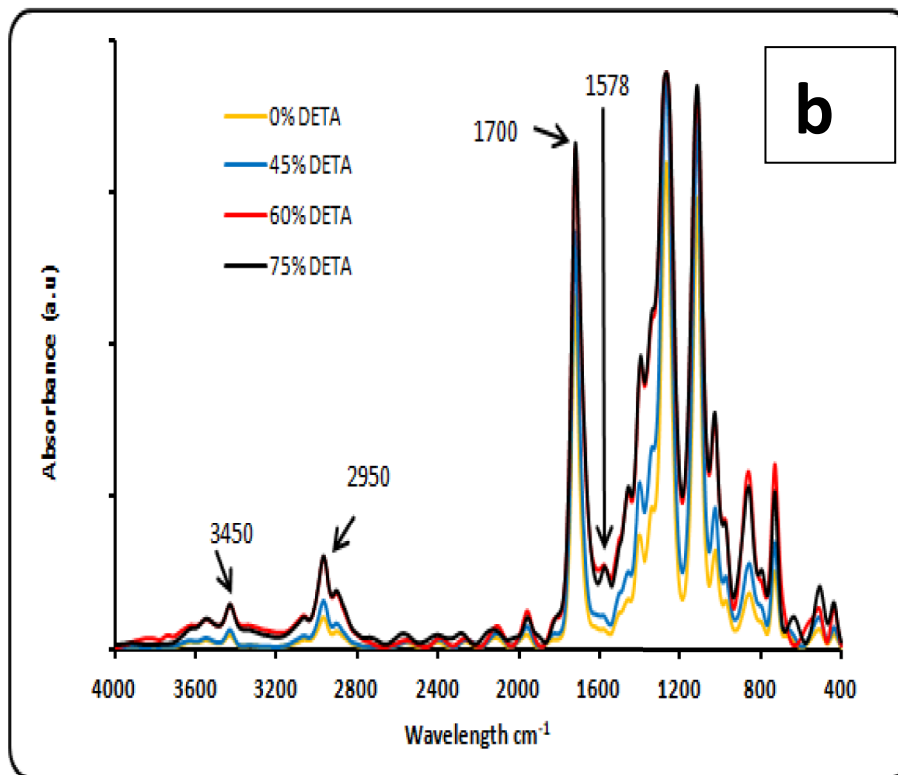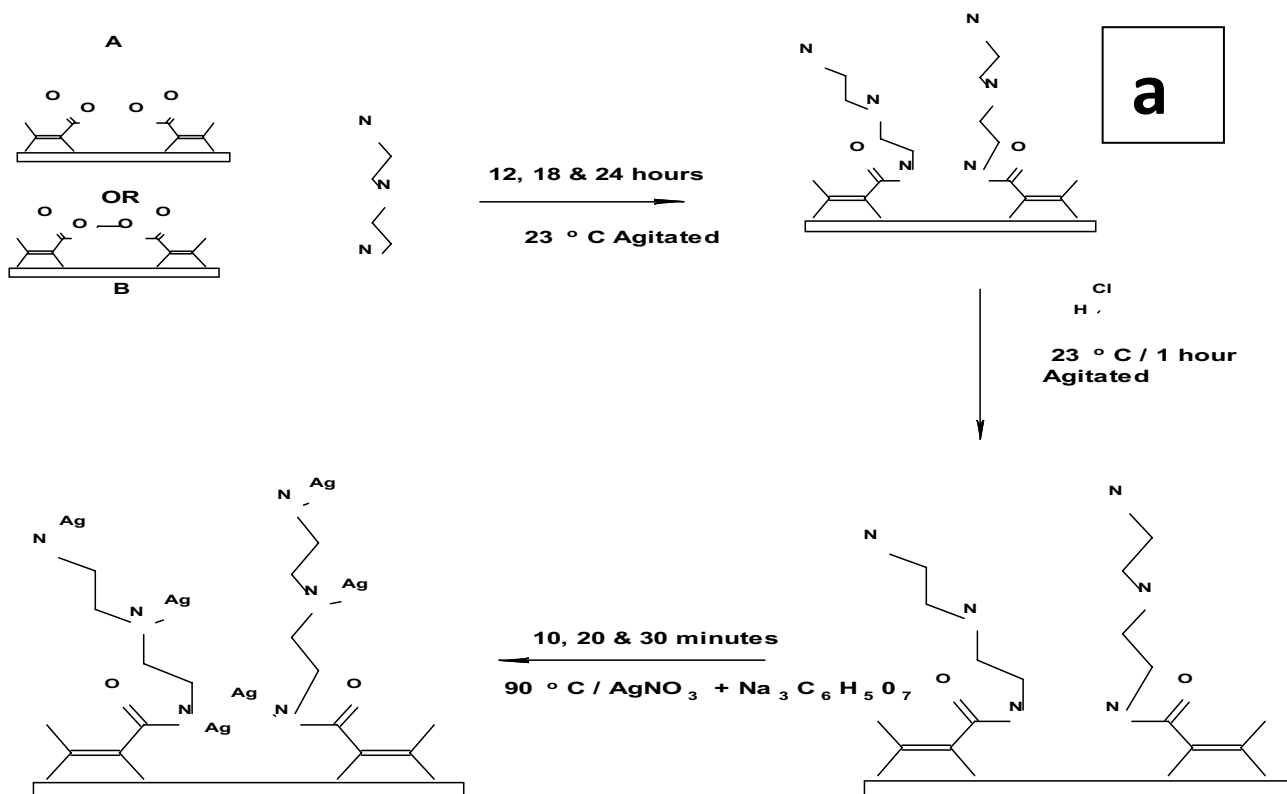
Fig. 1 **a** Proposed mechanism of modification of PET membrane with DETA and immobilisation of AgNPs on the modified surface and **b** FTIR spectra of unmodified PET membrane (CO-APET) and modi-fied PET membranes at 24-h reaction time and variable concentration of DETA of 75% (75A-PET), 60% (60A-PET), and 45% (45A-PET)

Table 2 XPS results showing elemental ratios of C1s and O1s of unmodified (0%DETA) and modified (75%DETA) PET membranes

PET membrane	Atomic ratios	
	Carbon (C1s)	Oxygen (O1s)
C0-APET	2.6	1
75%DETA	3.2	1

of samples 0%DETA and 75%DETA show that peaks of carbon (C1s), oxygen (O1s), and nitrogen (N1s) are in the binding energy regions of 285.21 eV, 532.63 eV, and 399.61 eV respectively.

The general survey graph for 0%DETA has no nitrogen peak, while that of 75%DETA has the nitrogen peak. The general survey graph of 75%DETA shows that nitrogen is present on the surface of the modified track-etched PET membrane. The binding energies in Fig. 2a and b agree with those reported in literature [41, 45]. The chemical states of nitrogen (N1s) and carbon (C1s) on the surface of PET membrane are represented in Fig. 2c and d; the chemical state graph for nitrogen (N1s) is from the sample 75%DETA. The chemical state graph for carbon (C1s) presents results for both samples 0%DETA and 75%DETA. The carbon (C1s) chemical state graph shows the chemical states of carbon when the PET membrane was not modified (sample

0%DETA) and the changes that occurred after modification of the track-etched PET membrane (sample 75%DETA).

Further to the general survey, the magnified N1s shell scan in Fig. 2c (NITROGEN) shows the chemical state of nitrogen on the surface of the modified PET membrane sample coded 75%DETA. The NITROGEN graph in Fig. 2c shows that the spectra peak for N1s is at a binding energy of 399.61 ($\approx$400) eV which is known to be for nitrogen in the chemical state of C-NH$_2$ [46]. Furthermore, the C1s shell scan in Fig. 2d (CARBON) shows the chemical states of carbon from samples 0%DETA and 75%DETA. The C1s shell scan shows three symmetrical peaks with binding energies at 284.9, 286.6, and 288.9 eV for the chemical states of C–C, C-O, and O-C=O respectively [47]. These C1s spectra peaks are characteristic peaks observed for polyethylene terephthalate polymers. The observed satellite peak π-π*, which is not so pronounced between 291 and 292 eV, is characteristic of polyethylene terephthalate polymer materials [46, 48]. The changes in binding energies that occurred as a result of changes in chemical state of carbon are tabulated in Table 3.

The amide bond formation gives rise to a change in the chemical state of carbon in O-C=O as observed in the reduction of the O-C=O peak height from 3428 to 2888 counts per second. The conspicuous change in C-O peak height is not expected; the expected observation would be the reduction in height of the C-O spectrum peak due to loss of glycol during the aminolysis reaction. This could be

Fig. 2 X-ray photoelectron spectroscopy general survey graphs of **a** unmodified PET (0%DETA) and **b** modified PET (75%DETA) showing elements within the detection limits, **c** XPS spectra of N1s peaks of amine-modified PET (NITROGEN), and **d** XPS spectra of C1s peaks for both unmodified (black) and amine-modified (red) PET membrane (CARBON)
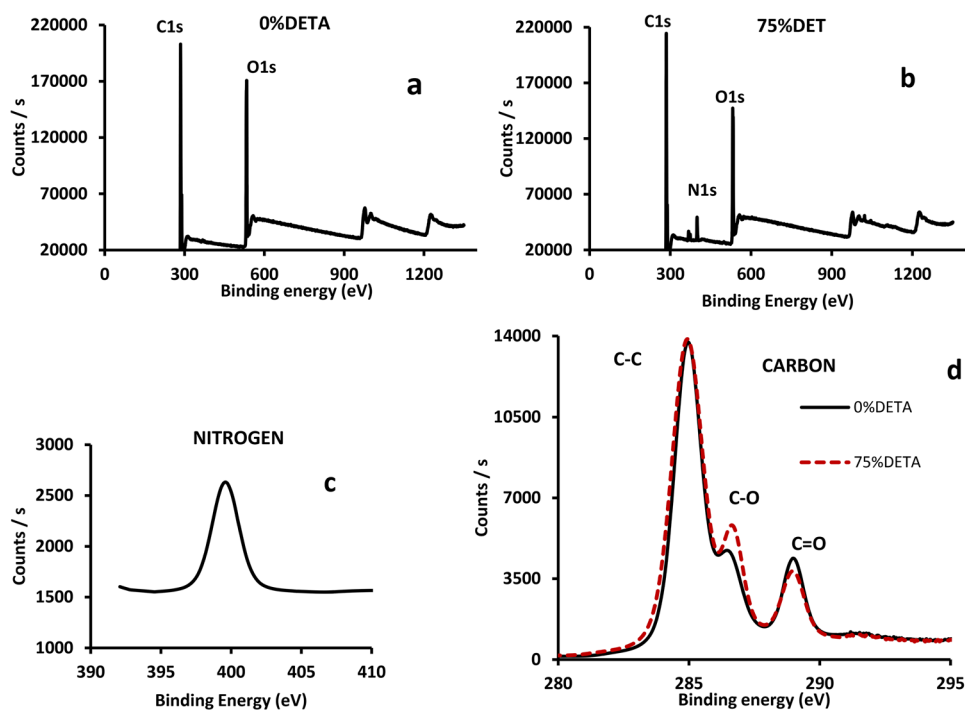
Table 3 Changes in peak heights of carbon chemical states

Chemical state of elements	Peak height (count/second)	
	0%DETA (PET)	75%DETA (Amine-PET)
C–C	13 158	13 362
C-O	3 209	4 226
O-C=O	3 428	2 888

contributed from atmospheric carbon existing in C-O chemical state during aminolysis reaction or storage.
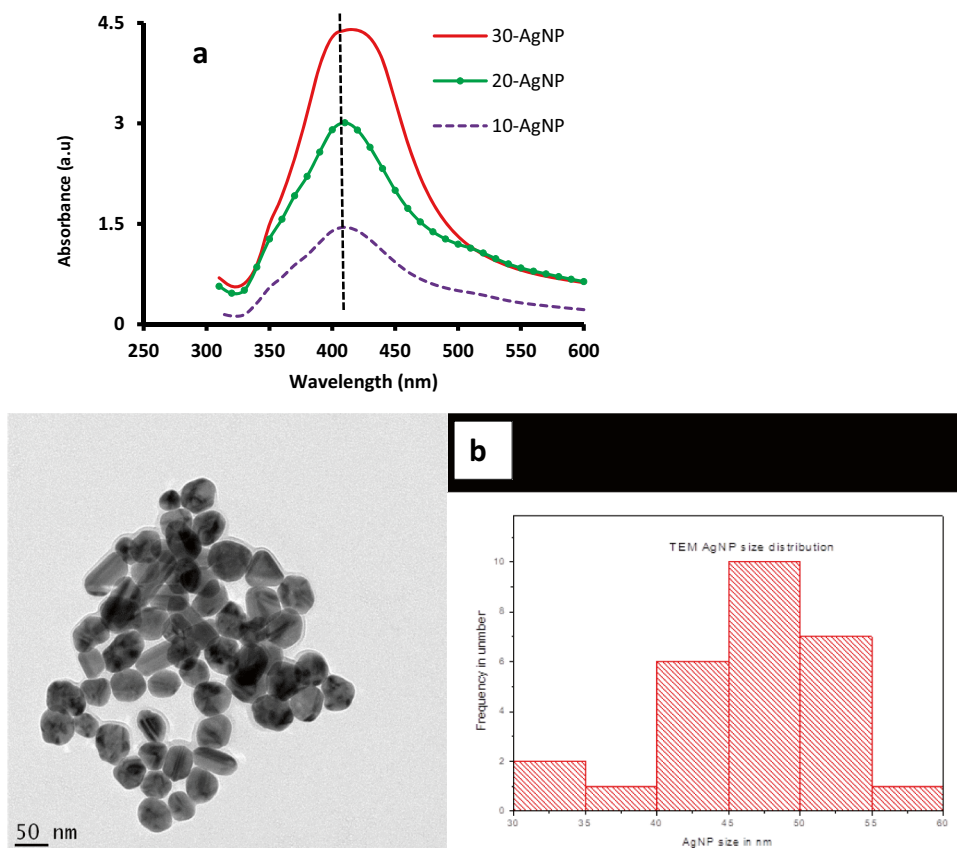
Silver nanoparticles

Silver nanoparticles were synthesized according to "Immobilization of AgNPs on PET membrane" without immersion of PET membrane in order to characterize the nanoparticle themselves. The UV–Vis spectroscopy results of synthesizing AgNPs at varied time of reaction after optimizing on temperature of reaction and concentration of trisodium citrate are shown in Fig. 3a. The variable parameter was time of reaction of 10 min, 20 min, or 30 min. The fixed parameters were the volume of 1% trisodium citrate of 2 mL and temperature of reaction at 90 °C.

The results in Fig. 3a show the increase in absorbance of the plasmonic peak height as the time of reaction was increased from 10 to 30 min. The results also show that plasmonic peak height had doubled after 20 min and tripled after 30 min. The results show that as the time was increased, the concentration of AgNPs increased as seen in the increase in peak height; this agrees with observations made by Kristavchuk et al. [18]. The narrowing of the plasmonic peaks with an increase in the time of reduction could be attributed to the formation of AgNPs within a narrow size range. The results show a trend that agrees with what has been reported in literature [23, 49].

The results of transmission electron microscopy for sample 20-AgNP are presented in Fig. 3b. Included in the results is the size distribution graph showing the spread of the sizes of AgNPs. The TEM image has an average silver nanoparticle size of 46.5 nm. The TEM image indicates that the majority of the AgNPs are spherical in shape with a few rod-like and triangular nanoparticle. The size distribution range of AgNPs was from 30 to 60 nm. The average size of

Fig. 3 **a** Ultraviolet–visible spectra of AgNPs synthesized at temperature of 90 °C and 2 mL volume of 1% trisodium citrate at varied times of 10 min (10-AgNP), 20 min (20-AgNP), and 30 min (30-AgNP) and **b** TEM image showing colloidal AgNPs synthesized for 20 min at 90 °C using 2 mL of 1% trisodium citrate (20-AgNP) and histogram showing the silver nanoparticle size distribution.

colloidal AgNPs of 46.5 is lower than reported by Taurozzi and Tarabara [50] for SERS application, which size was averaged at 58 nm.

Silver-coated PET membrane (SERS membrane)

Figure 4 shows scanning electron micrographs of nanoparticle silver-coated track-etched polyethene terephthalate membranes coded 10-AgPET, 20-AgPET, and 30-AgPET together with histograms showing size distribution of immobilized AgNPs. The SEM image of 10-AgPET shows AgNPs which are spherical in shape, and the corresponding histogram shows a nanoparticle size range of 28 to 44 nm. The histogram for sample 10-AgPET is asymmetric, skewed to the right, and has a high frequency of silver nanoparticle sizes between 36 and 40 nm. The average size of the AgNPs was 37.5 nm for sample 10-AgPET which was

immobilized for 10 min. For 20-AgPET, the image shows AgNPs which are spherical in shape and the corresponding histogram shows a nanoparticle size range of 40 to 62 nm. The histogram for sample 20-AgPET is symmetric and has a high frequency of silver nanoparticle sizes between 48 and 54 nm. The average size of AgNPs was 51.4 nm for the 20 min of immobilization (20-AgPET). 30-AgPET image shows AgNPs which are spherical in shape, and the corresponding histogram shows a nanoparticle size range of 54 to 68 nm. The histogram for sample 30-AgPET is asymmetric, partially skewed to the right and has a high frequency of silver nanoparticle sizes between 60 and 64 nm. The average size of the AgNPs was 62 nm for sample 30-AgPET which was immobilized for 30 min. The overall results show that the size of AgNPs increased relative to the increase in the time of immobilization of AgNPs on the surface of PET membrane [8].

Fig. 4 SEM images of silver-coated PET membrane prepared at 90 °C and with 2 mL of 1% trisodium citrate for samples of 10-AgPET (10 min), 20-AgPET (20 min), and 30-AgPET (30 min). The histograms of size distribution for silver-coated PET membranes for samples 10-AgPET (10 min), 20-AgPET (20 min), and 30-AgPET (30 min)
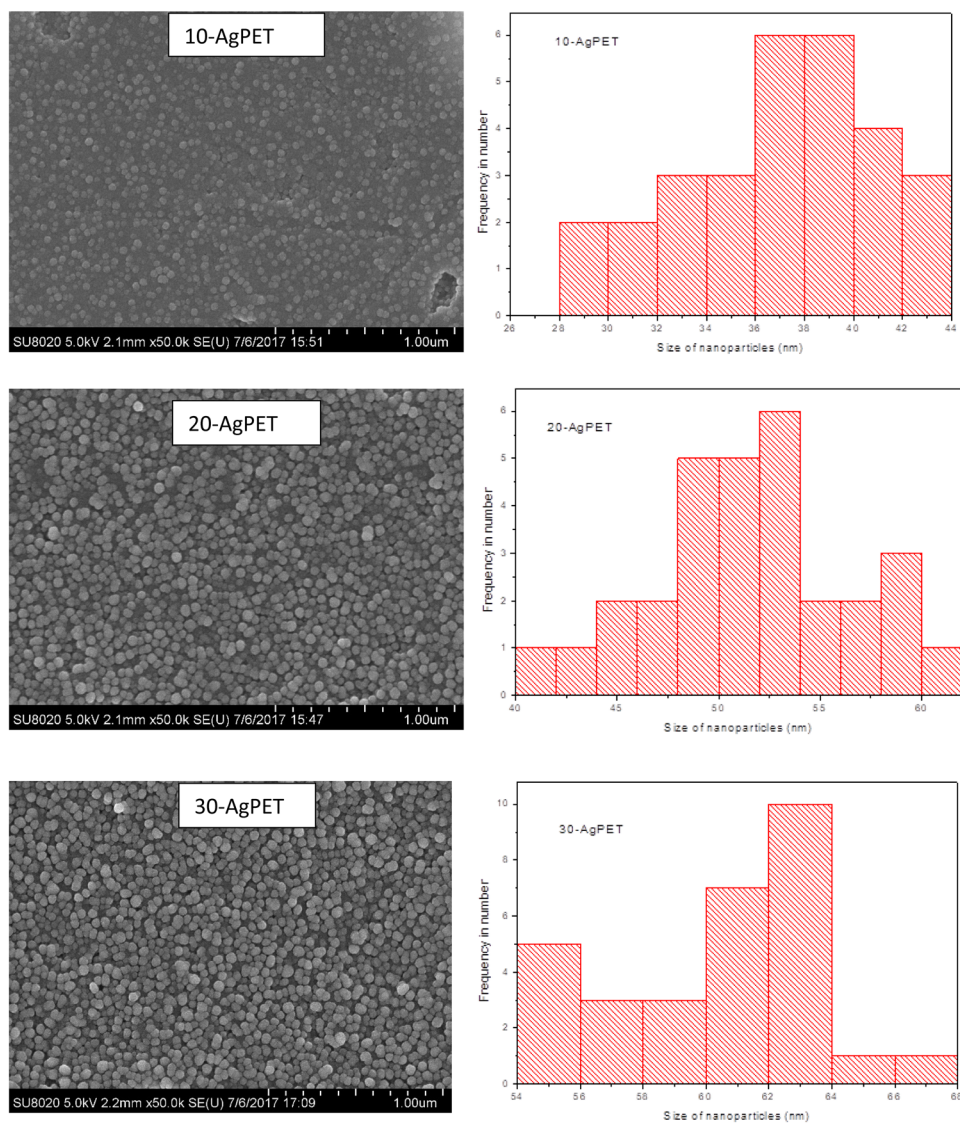
The UV–Vis spectroscopy results of the AgNPs coated PET membrane at varied time of reaction are shown in Fig. 5A. The results show an increase in the plasmonic peak height of silver-coated track-etched PET membranes. The sample 10-AgPET showed a small peak and sample 30-AgPET had the highest peak, whilst the rest were in between. The plasmonic peak heights showed a trend that increased from the sample that was immersed for 10 min (10-AgPET) to that for 30 min. The control sample Co-AgPET showed no plasmonic peak due to lack of AgNPs on the track-etched PET membrane surface. The trend in peak height agrees with literature where increasing the time of synthesis of AgNPs increases the number of nanoparticles [51]. The plasmonic peaks show a red shift as the

immobilization time increased from 10 to 30 min. The red shift, which is change in plasmonic peak position from short wavelength towards long wavelength meant that the size of AgNPs changed with an increase in the time of immobilization.

The immobilization of silver nanoparticles was done at different times in order to find the best conditions that would suppress the polyethene terephthalate Raman signal. Figure 5B shows the Raman spectra of the silver-coated track-etched PET membranes (10-AgPET, 20-AgPET, 30-AgPET) and the unmodified track-etched PET membrane (Co-AgPET) as a baseline (control sample).

The results for Raman spectra (Fig. 5B) show that as the time of silver nanoparticle immobilization increased, the

Fig. 5 **A** Ultraviolet–visible spectra of PET membranes coated at 90 °C and with 2 mL of 1% trisodium citrate for different immobilization times of 10 min (10-AgPET), 20 min (20-AgPET), 30 min (30-AgPET), and 0 min (Co-AgPET) and **B** Raman spectra of silver-coated track-etched PET membranes at reaction times (a) 10 min (10-AgPET), (b) 20 min (20-AgPET), and (c) 30 min (30-AgPET) and unmodified PET membrane (d) control (CO-AgPET) prepared at 90 °C using 2 mL of 1% trisodium citrate
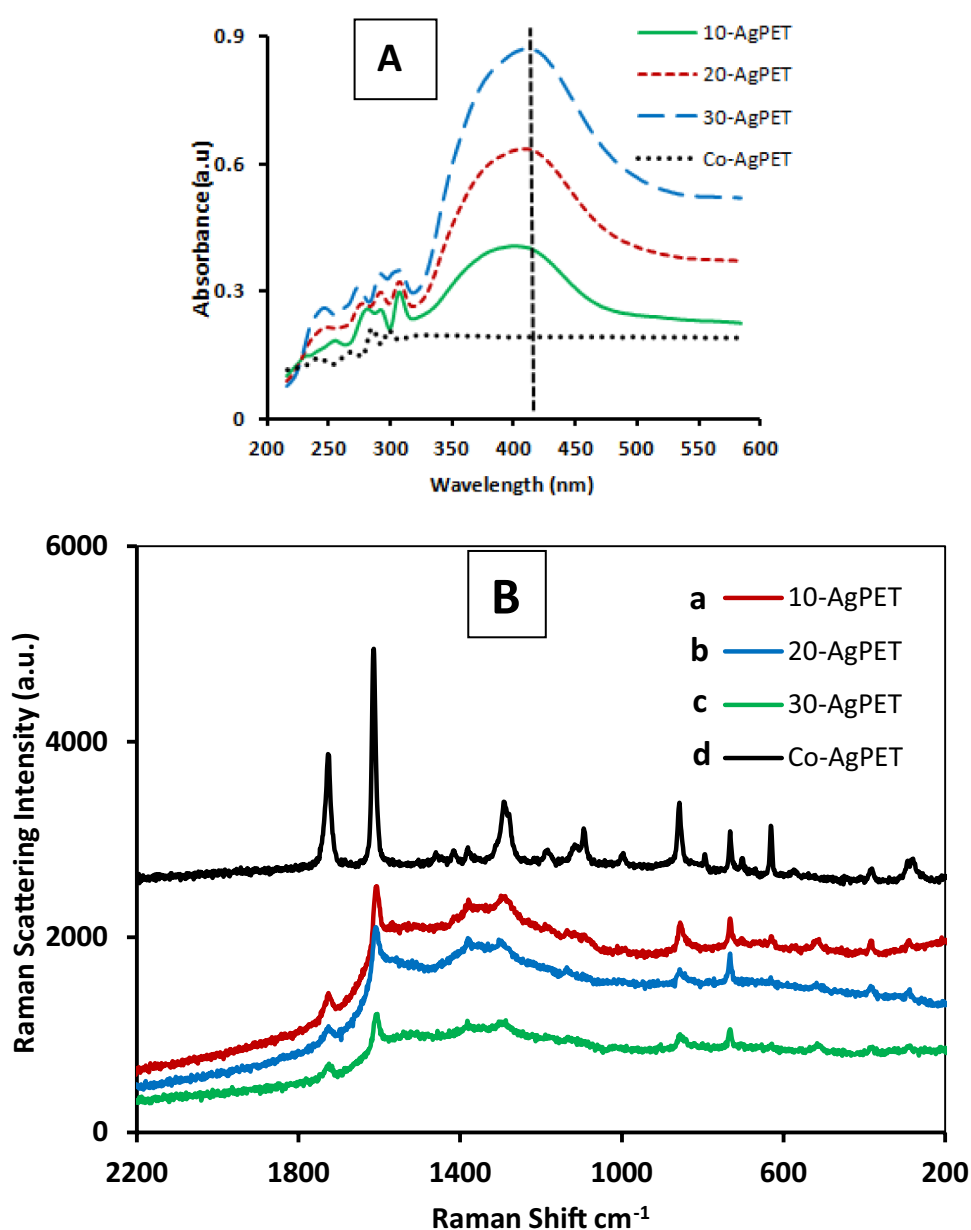
intensity of the peaks relating to the PET membrane were reduced with the lowest signal at 30 min as shown by the spectrum of 30-AgPET. The reduction of the PET peaks could be as a result of silver nanoparticles being coated on the PET membrane. The Raman spectra of silver-coated track-etched PET membranes (10-AgPET, 20-AgPET, 30-AgPET) show suppressed peaks relating to the polyethene terephthalate membrane, and these peaks were not as prominent as for the unmodified track-etched PET membrane (Co-AgPET). The reduction in the PET peak intensities follows the trend of time of silver nanoparticles immobilization on the surface of amine-modified track-etched PET membranes. The trend observed showed that as time of reduction reaction increased, so did the size of silver nanoparticles immobilized on the surface of PET. The silver-coated track-etched PET membrane coded 30-AgPET was therefore chosen as the most suitable platform for detection of acetaminophen using surface-enhanced Raman spectroscopy. The Raman spectrum of sample 30-AgPET was chosen as baseline because the silver-coated track-etched PET membrane showed the minimum peak intensities of the PET membrane itself. The cut-off point of immobilizing silver nanoparticles on modified track-etched PET membrane was set at 30 min because the size of silver nanoparticles of sample 30-AgPET fell within the average range of 58 nm as stated by Taurozzi and Tarabara [50].

Detection of acetaminophen using fabricated silver-coated track-etched polyethene terephthalate membrane as SERS platform

The moieties of acetaminophen have specific vibration modes that produce a Raman spectrum specific to acetaminophen [52]. The chemical structure of acetaminophen is shown in Fig. 6. Acetaminophen has functional groups which have peaks in its Raman spectrum, which are also common to other chemicals; the functional groups are phenyl, amide, carbonyl, and hydroxyl. Although acetaminophen has similar peaks to common functional groups, its overall Raman spectrum is specific to it only, giving its fingerprint signature. The typical acetaminophen peaks identified in its spectrum are outlined in Table 4 [52].

The peaks of the Raman spectrum in Table 4 were used to ascertain the presence of acetaminophen on the prepared surfaces of unmodified track-etched PET membrane (Co-AgPET), silver-coated track-etched PET membrane 30-AgPET, and a control surface made of silver and titanium oxide on a quartz support. Similar to Fourier transform infrared spectrum, a Raman spectrum comprises wavelength distribution of peaks equivalent in character to molecular vibrations specific to the analyte being characterized [53].

Surface-enhanced Raman spectroscopy (SERS), as an advanced Raman spectroscopy technique, was used to detect
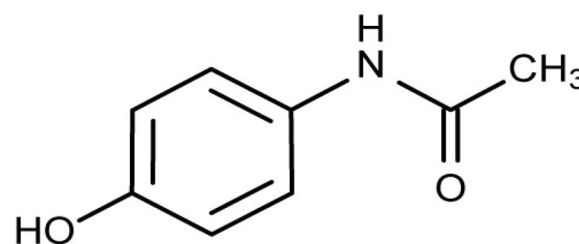

Fig. 6 Chemical structure of acetaminophen

acetaminophen using silver nanoparticles as SERS active materials to enhance the Raman signal. The detection of the molecules of acetaminophen on the silver-coated track-etched polyethene terephthalate membrane was carried out at ambient conditions. The Raman spectra of acetaminophen detected on the surface of silver-coated track-etched polyethene terephthalate (PET) membrane (30-AgPET), unmodified track-etched PET (Co-AgPET), and Quartz, a silver-coated glass surface (non-porous), are shown in Fig. 7A.

Figure 7A shows that the peak intensities are higher for the sample coded Quartz (a non-porous silver-coated glass) than that of 30-AgPET, the track-etched silver-coated track-etched PET membrane. In the case of the control sample, Co-AgPET, which is unmodified track-etched PET membrane, no characteristic peaks of acetaminophen could be observed among the overall prominent peaks of polyethene terephthalate membrane. This could be attributed to the lack of Ag nanoparticles to enhance the acetaminophen Raman fingerprint on the surface of sample Co-AgPET membrane. When comparing the Raman signal intensity of acetaminophen on sample Quartz (a non-porous SERS surface) against 30-AgPET (a track-etched silver-coated track-etched PET membrane), most of the SERS vibrational bands on the 30-AgPET sample are rather weak. The limited SERS intensity and the low spectral intensities could be ascribed to the loss of some molecules of acetaminophen that leach through the track etched PET pores, indicating that a smaller pore size of the track-etched PET could be more suitable to prevent loss of the analyte

Figure 7B shows that the intensity of the Raman peaks increased with an increase in acetaminophen concentration. The trend agrees with what was reviewed in the literature that Raman peak intensity is a function of the concentration

Table 4 Peaks in Raman spectrum of acetaminophen

Proposed bond	Spectral peak, cm^{-1}
C–O	854, 862, 1172
C–N	1234, 1245, 1281
C=C	1557, 1565, 1576
C=C	1611, 1615, 1623
C=O	1646, 1650
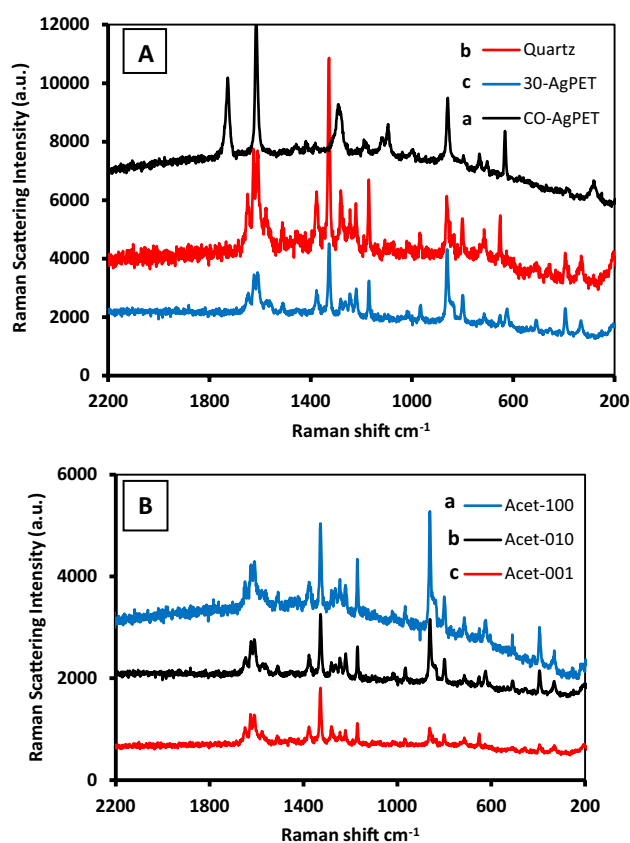
Fig. 7 **A** Raman spectra of 1.51 mg/L of acetaminophen on the surface of (a) Co-AgPET (unmodified track-etched PET) membrane, (b) quartz (Non-porous) membrane, and (c) 30-AgPET (silver-coated track-etched PET membrane). **B** Variation in Raman spectra intensity of different concentrations: (a) 15.1 mg/L, (b) 1.51 mg/L, and (c) 0.151 mg/L of acetaminophen in aqueous media

of analyte [50]. Sample Aceta-100, which is 15.1 mg/L, has its acetaminophen peak intensity greater than those of lower concentration (Aceta-010 and Aceta-001), which were 10 and 100 times diluted, respectively. The changes in the intensity of the peaks of the acetaminophen spectrum are consistently changing with a change in concentration. Theoretically, when there is a higher number of molecules on the surface-enhanced Raman spectroscopy (SERS) surface hot sites, there is a greater chance of observing medium to strong Raman signals [51]. This is also shown in peaks of the spectra in Fig. 7B

When more acetaminophen molecules covered the surface of silver-coated track-etched PET membrane, the possibility of observing a strong to medium Raman signal was greater. The SERS effect is provided by the localized surface plasmon of silver nanoparticles. The higher Raman scattering intensity could be as a result of SERS contributions from both electromagnetic effects and change transfer (chemical effects) arising from adsorption of acetaminophen molecules on the silver nanoparticles.

Application of spectra peaks for quantification

Theoretically, quantification of an analyte in a sample is possible with Raman spectroscopy since the Raman scattering is proportional to the concentration of the analyte. The intensity of Raman scattering of a vibration mode is directly proportional to vibrating moieties' concentration [54]. Raman spectra analysis could be used to extract information from the peak height or area, and/or use the ratio of peak height or area to quantify the analyte. This could be possible only if spectral peaks do not overlap, and all analyte samples are exposed to the same conditions to be affected equally by undetected interference. In reference to Fig. 7B showing Raman spectra of concentrations 15.10 mg/L, 1.51 mg/L, and 0.151 mg/L represented as Acet-100, Acet-010, and Acet-001 respectively, Fig. 8 shows the trend in specific Raman intensity peak heights (861, 1170, 1328, and 1608 cm^{-1}) relative to the concentration of acetaminophen.

The general trend in Fig. 8 shows that as the concentration increased so did the peak intensity height. The difference in the trends is observed when comparing the rate of change amongst the specific bonds. For instance, the rate of change of C=C (1608) and C-0 (1170) are not consistently correlated to an increasing concentration, but rates of change for C-O (1170) and C-N (1328) had a similar trend. The peak intensity trend for the C-O (861) vibration showed a trend response. The trend of peak intensity of the C-O bond versus the concentration had the best possible correlation of the two factors. The other bond vibrations C-O (1170), C-N (1328), and C=C (1608) showed no regular trend and if extrapolated towards zero concentration they crossed the peak intensity axis instead of the concentration axis.

The trend line of C-O (861) when extrapolated would give a limit of detection of approximately 0.0755 mg/L. The challenge with the peak intensity heights is that the
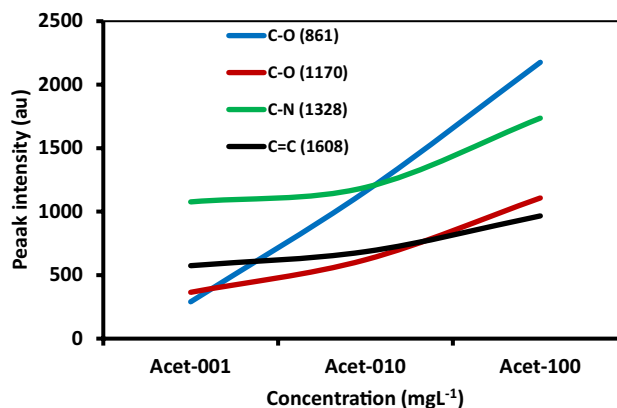
Fig. 8 Graphical presentation of relationship between concentration of acetaminophen and trends in Raman intensity peak height at specific bond vibrations

proportionality does not seem to be the same for all peak intensity heights; that is, the peak intensity increases were not the same for all spectrum peaks. The finding has not been reported anywhere else in literature, and therefore, this is the first observation to have been made by this study.

Conclusion

The modification of track-etched PET membranes with tri-amine at ambient room conditions was successfully achieved via a wet chemistry method. The modification of the surface of PET membrane was successfully confirmed by Fourier transform infrared and X-ray photoelectron spectroscopy. Silver nanoparticles were successfully immobilized on the chemically DETA-modified track-etched PET membrane. The use of diethylenetriamine provided sites on the surface of the inert polymer membrane on which AgNPs were immobilized. The Raman spectroscopy characterization of the silver-coated PET membrane showed that the more silver nanoparticles were deposited on the surface of amine-modified PET membrane. The silver-coated PET membrane fabricated after 30 min of nanoparticle immobilization successfully showed Raman spectra of acetaminophen when dropped and dried on the surface. The reported finding shows potential in the use of chemically immobilized AgNPs on the flexible PET membrane for various applications such as water treatment and biotechnology for antibacterial effect and, the use of AgNPs as surface-enhanced Raman spectroscopy substrates.

Declarations

Conflict of interest The authors declare no competing interests.

References

1. Lee A, Elam JW, Darling SB (2016) Membrane materials for water purification: design, development, and application. Environ Sci Water Res Technol 2:17–42
2. Li D, Zhai W, Li Y, Long Y (2014) Recent progress in surface enhanced Raman spectroscopy for the detection of environmental pollutants. Microchim Acta 181:23–43
3. Apel P (2001) Track etching technique in membrane technology. Radiat Meas 34:559–566
4. Bode-Aluko CA, Laatikainen K, Pereao O, Nechaev A, Kochnev I, Rossouw A, Dobretsov S, Branger C, Sarbu A, Petrik L (2019) Fabrication and characterisation of novel nanofiltration polymeric membrane. Mater Today Commun 20:100580
5. Bode-Aluko CA, Pereao O, Ndayambaje G, Petrik L (2017) Adsorption of toxic metals on modified polyacrylonitrile nanofibres: a review, Water, Air. Soil Pollution. https://doi.org/10.1007/s11270-016-3222-3
6. Bode-Aluko CA, Pereao O, Fatoba O, Petrik L (2017) Surface-modified polyacrylonitrile nanofibres as supports. Polym bull. https://doi.org/10.1007/s00289-016-1830-0
7. Goddard JM, Hotchkiss J (2007) Polymer surface modification for the attachment of bioactive compounds. Prog Polym Sci 32:698–725
8. Reznickova A, Kolska Z, Zaruba K, Svorcik V (2014) Grafting of gold nanoparticles on polyethyleneterephthalate using dithiol interlayer. Mater Chem Phys 145:484–490
9. Rossouw A, Kristavchuk O, Olejniczak A, Bode-Aluko C, Gorberg B, Nechaev A, Petrik L, Perold W, Apel P (2021) Modification of polyethylene terephthalate track etched membranes by planar magnetron sputtered Ti/TiO$_2$ thin films. Thin Solid Films 725:138641
10. Muthuvijayan V, Gu J, Lewis RS (2009) Analysis of functionalised polyethylene terephthalate with immobilized NTPDase and cysteine. Acta Biomater 5:3382–3393
11. Marchand-Brynaert J, Deldime M, Dupont I, Dewez J, Schneider Y (1995) Surface functionalisation of poly(ethylene terephthalate) film and membrane by controlled wet chemistry: Chemical characterisation of carboxylated surfaces. J Colloid Interface Sci 173:236–244
12. Drobota M, Persin Z, Zemljic L, Mohan T, Stana-Kleinschek K, Doliska A (2013) Chemical modification and characterisation of poly (ethylene terephthalate) surfaces for collagen immobilization. Open Chem 11:1786–1798
13. Fatiyants EK, Berezkin V, Kagramanov G (2013) Methods for modification of track-etched membranes designed for separation of biological objects. Pet Chem 53:471–481
14. Irena G, Jolanta B, Karolina Z (2009) Chemical modification of poly (ethylene terephthalate) and immobilization of the selected enzymes on the modified film. Appl Surf Sci 255:8293–8298
15. Caragheorgheopol A, Chechik V (2008) Mechanistic aspects of ligand exchange in gold nanoparticles. Phys Chem Chem Phys 10:5029–5041
16. Sperling RA, Parak WJ (2010) Surface modification, functionalisation and bioconjugation of colloidal inorganic nanoparticles, Philos. Trans. A. Math. Phys. Eng Sci 368:1333–1383
17. Braun GB, Lee SJ, Laurence T, Fera N, Fabris L, Bazan GC (2009) Generalized approach to SERS nanomaterials via controlled nanoparticle linking, polymer encapsulation, and small-molecule infusion. J Phys Chem C 113:13622–13629
18. Kristavchuk OV, Nikiforov IV, Kukushkin VI, Nechaev AN, Apel PY (2017) Immobilization of silver nanoparticles obtained by electric discharge method on a track membrane surface. Colloid J 79:637–646
19. Meng X, Tang S, Vongehr S (2010) A review on diverse silver nanostructures. J Mater Sci Technol 26:487–522
20. Khodashenas B, Ghorbani HR (2015) Synthesis of silver nanoparticles with different shapes. Arab J Chem 1–16
21. Abou-El-Nour KM, Eftaiha A, Al-Warthan A, Ammar RA (2010) Synthesis and applications of silver nanoparticles. Arab J Chem 3:135–140
22. Sharma VK, Yngard RA, Lin Y (2009) Silver nanoparticles: Green synthesis and their antimicrobial activities. Adv Colloid Interface Sci 145:83–96

23. Smyth C, Mirza I, Lunney J, McCabe E (2013) Surface-enhanced Raman spectroscopy (SERS) using silver nanoparticle films produced by pulsed laser deposition. Appl Surf Sci 264:31–35

24. Khan Z, Al-Thabaiti SA, Obaid AY, Al-Youbi A (2011) Preparation and characterisation of silver nanoparticles by chemical reduction method. Colloids Surf B: Biointerfaces 82:513–517

25. Patil RS, Kokate MR, Jambhale CL, Pawar SM, Han SH, Kolekar SS (2012) One-pot synthesis of PVA-capped silver nanoparticles their characterisation and biomedical application. Adv Nat Sci Nanosci Nanotech 3:1–7

26. Boujday S, de la Chapelle ML, Srajer J, Knoll W (2015) Enhanced vibrational spectroscopies as tools for small molecule biosensing. Sensors 15:21239–21264

27. Craig AP, Franca AS, Irudayaraj J (2013) Surface-enhanced Raman spectroscopy applied to food safety. Annu Rev Food Sci Technol 4:369–380

28. Halvorson RA, Vikesland PJ (2010) Surface-enhanced Raman spectroscopy (SERS) for environmental analyses. Environ Sci Technol 44:7749–7755

29. Hering K, Cialla D, Ackermann K, Dörfer T, Möller R, Schneidewind H (2008) SERS: A versatile tool in chemical and biochemical diagnostics. Anal Bioanal Chem 390:113–124

30. Le Ru E, Etchegoin P (2008) Principles of surface-enhanced Raman spectroscopy: and related plasmonic effects. Elsevier, Oxford

31. Lucotti A, Zerbi G (2007) Fiber-optic SERS sensor with optimized geometry. Sens Actuators B: Chemical 121:356–364

32. Huh YS, Chung AJ, Erickson D (2009) Surface enhanced Raman spectroscopy and its application to molecular and cellular analysis. Microfluid Nanofluid 6:285–297

33. Zhang Y, Yu W, Pei L, Lai K, Rasco B, Huang Y (2015) Rapid analysis of malachite green and leucomalachite green in fishmuscles with surface-enhanced resonance Raman scattering. Food chem 169:80–84

34. Ma P, Liang F, Wang D, Yang Q, Cao B, Song D (2015) Selective determination of o-phenylenediamine by surface-enhanced Raman spectroscopy using silver nanoparticles decorated with α-cyclodextrin. Microchim Acta 182:167–174

35. Cialla D, März A, Böhme R, Theil F, Weber K, Schmitt M (2012) Surface-enhanced Raman spectroscopy (SERS): Progress and trends. Anal Bioanal Chem 403:27–54

36. Botti S, Cantarini L, Almaviva S, Puiu A, Rufoloni A (2014) Assessment of SERS activity and enhancement factors for highly sensitive gold coated active materials probed with explosive molecules. Chem Phys Lett 592:277–281

37. Péron O, Rinnert E, Lehaitre M, Crassous P, Compère C (2009) Detection of polycyclic aromatic hydrocarbon (PAH) compounds in artificial sea-water using surface-enhanced Raman scattering (SERS). Talanta 79:199–204

38. Costa J, Sant'Ana A, Corio P, Temperini M (2006) Chemical analysis of polycyclic aromatic hydrocarbons by surface-enhanced Raman spectroscopy. Talanta 70:1011–1016

39. Muehlethaler C, Leona M, Lombardi JR (2015) Review of surface enhanced Raman scattering applications in forensic science. Anal Chem 88:152–169

40. Rao R, Manu B, Kumar A (2017) Behavioral, physical and biochemical responses of Cyprinus Carpio for paracetamol exposure. Inter Jour Emerg Res in Manag & Techn 6:2278–9359

41. Andrade GF, Fan M, Brolo AG (2010) Multilayer silver nanoparticles-modified optical fiber tip for high performance SERS remote sensing. Biosens Bioelectron 25:2270–2275

42. Lee PC, Meisel D (1982) Adsorption and surface-enhanced Raman of dyes on silver and gold sols. J Phys Chem 86:3391–3395

43. Xue L, Lu Y (2013) Electroless copper plating on 1, 2-ethylenediamine grafted poly (ethyleneterephthalate) for the fabrication of flexible copper clad laminate. J Mater Sci Mater Electron 24:2211–2217

44. Noel S, Liberelle B, Yogi A, Moreno MJ, Bureau MN, Robitaille L (2013) A non-damaging chemical amination protocol for poly (ethylene terephthalate)–application to the design of functionalised compliant vascular grafts. J Mater Chem B 1:230–238

45. Awasthi K, Choudhury S, Komber H, Simon F, Formanek P, Sharma A (2014) Functionalisation of track-etched poly (ethylene terephthalate) membranes as a selective filter for hydrogen purification. Int J Hydrog Energy 39:9356–9365

46. Vesel A, Junkar I, Cvelbar U, Kovac J, Mozetic M (2008) Surface modification of polyester by oxygen-and nitrogen-plasma treatment. Surf interface anal 40:1444–1453

47. Makiabadi T, Bouvrée A, Le Nader V, Terrisse H, Louarn G (2010) Preparation, optimization, and characterisation of SERS sensor active materials based on two-dimensional structures of gold colloid. Plasmonics 5:21–29

48. Basri H, Ismail AF, Aziz M (2011) Polyethersulfone (PES)–silver composite UF membrane: Effect of silver loading and PVP molecular weight on membrane morphology and antibacterial activity. Desalination 273:72–80

49. Kruszewski S, Cyrankiewicz M (2011) Activation of silver colloids for enhancement of Raman scattering. Acta Phys Pol A 119:1018–1022

50. Taurozzi JS, Tarabara VV (2007) Silver nanoparticle arrays on track etch membrane support as flow-through optical sensors for water quality control. Environ Eng Sci 24:122–137

51. Solov'ev AY, Potekhina T, Chernova I, Basin BY (2007) Track membrane with immobilized colloid silver nanoparticles. Russ J Appl Chem 80:438–442

52. Kauffman JF, Batykefer LM, Tuschel DD (2008) Raman detected differential scanning calorimetry of polymorphic transformations in acetaminophen. J pharm Biomed Anal 48:1310–1315

53. Ferraro JR (2003) Introductory Raman spectroscopy. Academic press, New York

54. Strachan CJ, Rades T, Gordon KC, Rantanen J (2007) Raman spectroscopy for quantitative analysis of pharmaceutical solids. J Pharm Pharmacol 59:179–192

Terms and Conditions